Journal of Modern Optics
Publication details, including instructions for authors and subscription information:
http://www.informaworld.com/smpp/title~content=t713191304

Performance of line codes in optical direct detection continuous phase frequency shift keying transmission system impaired by polarization mode dispersion

M. S. Islam [a]; S. P. Majumder [a]
[a] Department of Electrical and Electronic Engineering, Bangladesh University of Engineering and Technology, Dhaka, Bangladesh

Online Publication Date: 01 October 2008

To cite this Article Islam, M. S. and Majumder, S. P.(2008)'Performance of line codes in optical direct detection continuous phase frequency shift keying transmission system impaired by polarization mode dispersion',Journal of Modern Optics,55:18,3001 — 3011

To link to this Article: DOI: 10.1080/09500340802296315

URL: http://dx.doi.org/10.1080/09500340802296315

Journal of Modern Optics
Vol. 55, No. 18, 20 October 2008, 3001–3011

Performance of line codes in optical direct detection continuous phase frequency shift keying transmission system impaired by polarization mode dispersion

M.S. Islam* and S.P. Majumder

Department of Electrical and Electronic Engineering, Bangladesh University of Engineering and Technology, Dhaka, Bangladesh

(*Received 29 January 2008; final version received 20 June 2008*)

Small deviations from perfect circular symmetry in the core region of single mode fiber (SMF) cause optical pulses to become broadened as they propagate. This phenomenon is referred to as polarization mode dispersion (PMD), which leads to intersymbol interference and becomes a major impediment for the high speed long-haul fiber-optic links. We present here the theoretical complement for evaluating the performance of a line-coded continuous phase frequency shift keying (CPFSK) optical transmission system with a direct detection receiver. The analysis is carried out for two different line-coding schemes, i.e. alternate mark inversion (AMI) and order-1 coding, to investigate the effectiveness of the line coding in counteracting the effect of PMD in a CPFSK direct detection transmission system in the presence of group velocity dispersion (GVD) and receiver noise in a single mode fiber. The average bit error rate (BER) performances are evaluated without and compared to that of line codes at a bit rate of $10\,\mathrm{Gb\,s^{-1}}$ considering Maxwellian distribution for the mean differential group delay (DGD). We found that the amount of power penalty improvement of line-coded systems is within 0.65 to 2.25 dB with respect to NRZ data at a BER of 10^{-9}.

Keywords: line code; differential group delay; polarization mode dispersion; bit error rate; continuous phase frequency shift keying and probability density function

1. Introduction

Today the vast majority of long distance telecommunications and Internet traffic is carried by an optical fiber communication system. As the bit rate of an optical transmission system and networks increases to $10–40\,\mathrm{Gb\,s^{-1}}$ and beyond, signal degradation due to PMD effects may become significant [1,2]. It is anticipated that the performance of a long-haul $40\,\mathrm{Gb\,s^{-1}}$ system would be limited by PMD. In a linear

*Corresponding author. Email: mdsaifulislam@iict.buet.ac.bd

ISSN 0950–0340 print/ISSN 1362–3044 online

DOI: 10.1080/09500340802296315
http://www.informaworld.com

dispersive medium, the PMD effects are well described by the PMD vector, whose direction is along a principal state of polarization (PSP) and whose magnitude corresponds to the DGD between two PSPs. With the ever increasing bit rate in optical transmission systems, much effort has been spent on understanding PMD impairments and developing PMD mitigation techniques [3–6]. Due to the stochastic nature of PMD and the fact that all the orders of PMD are bound together, it is not trivial to evaluate PMD penalties and compensate for PMD impairments. To overcome PMD limitations, many PMD mitigation techniques have been proposed and demonstrated, including PMD tolerant modulation formats [7–9], electronic equalization techniques and optical PMD compensation [10,11]. PMD tolerant modulation formats or passive techniques do not require any dynamically adjusted components and are bit rate independent. It includes use of more PMD robust line-coded signal and soliton transmission, allocating more margins to PMD distortions, forward error correction coding, channel switching and polarization scrambling.

Optical CPFSK is an attractive modulation format as it permits generation of compact spectra that allows for receiver detection by properly selecting the modulation index [12]. In this paper, we present a theoretical analysis for evaluating the performance of a line-coded CPFSK optical transmission system with a direct detection receiver. The analysis is carried out for AMI and order-1 to find the efficacy of the line-coding in tolerating the effect of PMD in a CPFSK optical transmission system. The average BER performance results are evaluated with line codes and compared with the NRZ-CPFSK system at a bit rate of $10\,\mathrm{Gb\,s^{-1}}$ considering Maxwellian probability distribution for the mean DGD due to PMD. Finally, we compared the performance of the two line-codes with NRZ format in counteracting the PMD effects.

2. System model

Figure 1(*a*) shows the random NRZ data process representing the information signal that is passed through a linecoder to shape the information signal spectrum. Two different line-coding techniques, i.e. AMI and order-1 coding are considered in this work. The line-coded data is used to modulate the DBF laser to generate the CPFSK signal. The low pass equivalent CPFSK system model considering PMD and chromatic dispersion is shown in Figure 1(*b*). The signal components in the two output PSPs propagate independently through the entire system from the modulator to the balanced receiver. In the transmitter, non-return to zero (NRZ) data at $10\,\mathrm{Gb\,s^{-1}}$ is used to directly modulate a laser to generate the CPFSK signal that is transmitted through a single mode fiber. At the receiving end, a MZI-based direct detection receiver detects the received optical signal. The fields corresponding to the two PSPs are separately detected and the resulting photocurrents are summed. We decompose the entire system into a pair of subsystems, each corresponding to one PSP. We sum the outputs of the two subsystems to obtain sampled decision variables $i_m(t) = i_{m1}(t) + i_{m2}(t)$. The output photocurrent is filtered by a low pass filter and fed to a sampler followed by a comparator. The threshold voltage of the comparator is set to zero value. If the output voltage is greater than zero a binary '1' is detected, otherwise a binary '0' is detected.

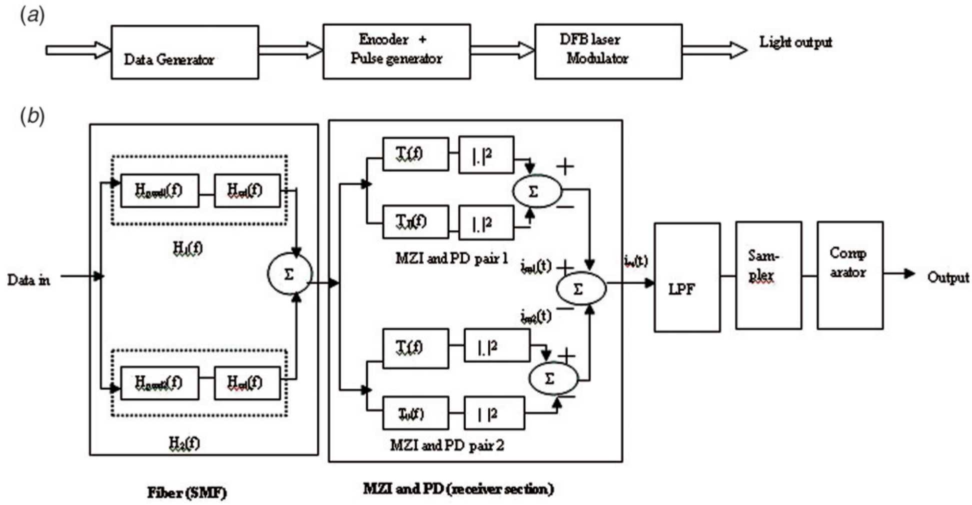

Figure 1. (*a*) Block diagram of the optical linecoded pulse generation. (*b*) Low pass equivalent direct detection CPFSK system model considering PMD and chromatic dispersion. (The color version of this figure is included in the online version of the journal.)

3. Theoretical analysis

The complex electric field at the output of the CPFSK transmitter and input to the fiber is represented as

$$E_1(t) = (2P_{\mathrm{T}})^{1/2} \exp[\mathrm{j}\{2\pi f_{\mathrm{c}} t + \phi_{\mathrm{s}}(t)\}][c_1 \cdot e_1], \tag{1}$$

$$E_2(t) = (2P_{\mathrm{T}})^{1/2} \exp[\mathrm{j}\{2\pi f_{\mathrm{c}} t + \phi_{\mathrm{s}}(t)\}][c_2 \cdot e_2], \tag{2}$$

where f_{c} is the carrier frequency, P_{T} is the transmitted optical power and the CPFSK modulating phase $\phi_{\mathrm{s}}(t)$ is given by

$$\phi_{\mathrm{s}}(t) = 2\pi\Delta f \int_{-\infty}^{t} \sum_{k=-\infty}^{\infty} a_k p(t - kT)\mathrm{d}t + \phi_{\mathrm{n}}(t), \tag{3}$$

where a_k is the random NRZ bit, Δf is the peak frequency deviation, $p(t)$ is the elementary pulse shape and $\phi_{\mathrm{n}}(t)$ is the phase noise of the transmitting laser. Here c_1, c_2 represent unit vectors and e_1, e_2 represent the two principal states of polarization, respectively. The electric field at the output of the fiber is then given by

$$E_{01}(t) = (2P_{\mathrm{T}})^{1/2} \exp[\mathrm{j}\{2\pi f_{\mathrm{c}} t + \phi_{\mathrm{s}}(t)\}][c_1 \cdot e_1] \otimes h_1(t), \tag{4}$$

$$E_{02}(t) = (2P_{\mathrm{T}})^{1/2} \exp[\mathrm{j}\{2\pi f_{\mathrm{c}} t + \phi_{\mathrm{s}}(t)\}][c_2 \cdot e_2] \otimes h_2(t), \tag{5}$$

where $h_1(t)$ and $h_2(t)$ are the inverse Fourier transform of the fiber transfer function $H_1(f)$ and $H_2(f)$, respectively, which include the effect of PMD and GVD and $\otimes$ denotes convolution. The low pass equivalent expression for $H_1(f)$ and $H_2(f)$ are given by [13]

$$H_1(f) = \alpha^{1/2} \exp\left[j2\pi f\left(-\frac{\Delta\tau}{2} \right) - j\gamma(\pi f T)^2 \right], \tag{6}$$

$$H_2(f) = (1-\alpha)^{1/2} \exp\left[j2\pi f\left(\frac{\Delta\tau}{2} \right) - j\gamma(\pi f T)^2 \right], \tag{7}$$

where $\Delta\tau$ represents the DGD between the two PSPs, α is the PMD power-splitting ratio and $\gamma = (\lambda^2/\pi c)DR_bL$ is the chromatic dispersion index. Here we assume that there is negligible polarization-dependent loss and we use the principal states model to characterize first-order PMD.

After detection of the two CPFSK polarization state signals, the output electric fields at the output of the low pass filter can be written as

$$E_{01}(t) = (2P_s)^{1/2} \exp[j\{2\pi f_c t + \phi_{s1}(t) + \theta_{n1}(t)\}][c_1 \cdot e_1], \tag{8}$$

$$E_{02}(t) = (2P_s)^{1/2} \exp[j\{2\pi f_c t + \phi_{s2}(t) + \theta_{n2}(t)\}][c_2 \cdot e_2]. \tag{9}$$

The output modulation phase ($\phi_{s1}(t)$ or $\phi_{s2}(t)$) of the low-pass signal resulting from filtering with symmetric low-pass filter (bandwidth B) with equivalent low-pass impulse response $h'(t)$ is given by [14,15]

$$\phi_s(t) = \int_{-\infty}^{\infty} h'(\tau)\varphi(t-\tau)\mathrm{d}\tau + \sum_{n=1}^{\infty} \frac{(-1)^n}{(2n+1)!} f_{2n+1}(t), \tag{10}$$

where the explicit expression for $f_k(t)$ can be found in [14]. The output phase of the low-pass signal is thus the sum of a term that represents linear filtering of the input phase and other terms representing various orders of distortion introduced by the filter. In the absence of phase noise, if $\phi_{sl}(t)$ denotes the leading term in the expansion (10), the normalized mean square error (MSE) defined as $\mathrm{MSE} = E[\phi_s(t) - \phi_{sl}(t)]^2/E[\phi_{sl}(t)]^2$, and as evaluated as following [15], for NRZ and AMI with a Butterworth filter ($BT = 2$), is found to be less than 10^{-4} for both flat and nonflat frequency modulation characteristics. In the presence of phase noise, the above assumptions are also valid for a narrowband CPFSK system [15,16]. With the demodulation time $\tau = T/2h$, $h \leq 1$ (narrowband CPFSK) and the symmetric low-pass filter, the correlation between combined phase noise $\theta_n(t)$ and $\theta_n(t-\tau)$ is zero. This justifies that $\phi_s(t)$ in (10) can be well approximated by $\phi_{sl}(t)$, which is linear. We can, therefore, write the output phase of the low-pass filters for two polarization state signals as

$$\begin{aligned} \phi_{s1}(t) &= \mathrm{Re}\,[\varphi(t) \otimes h_1'(t)] \\ &= 2\pi\Delta f \int_{-\infty}^{t} \sum_k a_k \,\mathrm{Re}\,[p(t-kT) \otimes h_1'(t)]\mathrm{d}t, \end{aligned} \tag{11}$$

$$\begin{aligned}\phi_{s2}(t) &= \mathrm{Re}\,[\varphi(t)\otimes h_2'(t)]\\ &= 2\pi\Delta f\int_{-\infty}^{t}\sum_k a_k\,\mathrm{Re}\,[p(t-kT)\otimes h_2'(t)]\mathrm{d}t,\end{aligned} \tag{12}$$

where $h_1'(t)$ and $h_2'(t)$ are impulse responses of the low-pass filters.

3.1. *CPFSK with NRZ data*

In the case of random NRZ data $\sum_{k=-\infty}^{\infty} a_k p(t-kT)$, where $a_k = \pm 1$ represents the kth information bit and $p(t)$ is a rectangular pulse of unit amplitude and duration T seconds. In the FSK direct detection receiver with Mach–Zehnder interferometer (MZI), the MZI acts as an optical discriminator and differentially detects the 'mark' and 'space' of the received FSK signal, which are then directly fed to a pair of photo-detectors. The transmittances of the two branches of the MZI are $T_{\mathrm{I}}(f)$ and $T_{\mathrm{II}}(f)$, and τ is the time delay between the two branches.

For a 'mark' transmission and ideal CPFSK demodulation condition (assuming NRZ data), we have $2\pi f_c\tau = (2n+1)(\pi/2)$, where n is an integer; and $2\pi\Delta f_\tau = \pi/2$. Thus, the currents at the output of the photo-detectors can be expressed as

$$i_{m1}(t) = R_d P_s \cos\left[2\pi f_c\tau + \frac{\pi}{2} - \frac{\pi}{2} + \frac{\pi}{2}q_1(t) + \frac{\pi}{2}\sum_{k\neq 0} a_k q_1(t-kT) + \Delta\theta_{n1}(t,\tau)\right][c_1\cdot e_1], \tag{13}$$

$$i_{m2}(t) = R_d P_s \cos\left[2\pi f_c\tau + \frac{\pi}{2} - \frac{\pi}{2} + \frac{\pi}{2}q_2(t) + \frac{\pi}{2}\sum_{k\neq 0} a_k q_2(t-kT) + \Delta\theta_{n2}(t,\tau)\right][c_2\cdot e_2], \tag{14}$$

where

$$q_1(t) = \frac{1}{\tau}\int_{t-\tau}^{t} g_1(t)\mathrm{d}t; \quad q_2(t) = \frac{1}{\tau}\int_{t-\tau}^{t} g_2(t)\mathrm{d}t \tag{15}$$

and

$$g_1(t) = \mathrm{Re}[p(t)\otimes h_1'(t)]; \quad g_2(t) = \mathrm{Re}[p(t)\otimes h'_2(t)]. \tag{16}$$

The current at the output of the photo-detectors (for a 'mark' transmission) can be expressed, following [17], as

$$i_m(t) = 2R_d P_s[\cos(\delta\varphi)\cos(\Delta\varphi)] + n(t). \tag{17}$$

If we consider the mean phase distortion only then the conditional bit error rate can be expressed as

$$P(e|\delta\varphi, \Delta\varphi) = \frac{1}{2}\,\mathrm{erfc}\big(Q/2^{1/2}\big), \tag{18}$$

where

$$Q = \frac{i_m(t)}{\sigma_m}. \tag{19}$$

For a given value of differential group delay (DGD) $\Delta\tau$, the conditional BER can be expressed as [14]

$$\mathrm{BER}(\Delta\tau) = \int_{-\infty}^{\infty}\int_{-\infty}^{\infty} P(e|\delta\varphi, \Delta\varphi) P_{\delta\varphi}(\delta\varphi) P_{\Delta\varphi}(\Delta\varphi)\, \mathrm{d}(\delta\varphi)\mathrm{d}(\Delta\varphi), \tag{20}$$

where $P_{\delta\varphi}(\delta\varphi)$, $P_{\Delta\varphi}(\Delta\varphi)$ are the pdf of the random output phase fluctuation $\delta\varphi$ and $\Delta\varphi$, respectively, due to an intersymbol interference bit pattern caused by PMD and GVD.

Although the mean DGD for an installed fiber is constant, changing environmental factors (e.g. temperature, pressure, vibration etc.) causes the instantaneous DGD, $\Delta\tau(\lambda, t)$, at given wavelength to vary about the mean. The DGD for a given wavelength at any moment in time $\Delta\tau(\lambda, t)$ is a random variable with a Maxwellian probability density function (pdf) and given by [18]

$$P_{\Delta\tau}(\Delta\tau) = \frac{32\Delta\tau^2}{\pi^2\langle\Delta\tau\rangle^3}\exp\left(-\frac{4\Delta\tau^2}{\pi\langle\Delta\tau\rangle^2}\right), \quad \Delta\tau > 0, \tag{21}$$

where $\langle\Delta\tau\rangle$ is the quadratic mean of the instantaneous DGD, $\Delta\tau$. So, the average bit error probability can be evaluated as

$$\mathrm{BER}(\langle\Delta\tau\rangle) = \int_{-\infty}^{\infty} \mathrm{BER}(\Delta\tau) P_{\Delta\tau}(\Delta\tau)\mathrm{d}(\Delta\tau). \tag{22}$$

3.2. *CPFSK with line-coding*

As mentioned earlier, appropriate line-coding of the DBF laser driving signal can overcome the adverse effects of PMD. In this work we have considered two types of line-coding scheme, i.e. AMI and order-1. Our main goal is to study the relative effectiveness of these two line codes in overcoming the pulse dispersion performance degradation caused by PMD. The linecoder shown in Figure 1(a) can be viewed as a linear time-invariant filter that acts on the input data signal of (3) to generate an output sequence of data given by

$$I'(t) = \sum_{k=-\infty}^{\infty} b_k r(t - kT), \tag{23}$$

where b_k's are independent and identically distributed (iid) random variables taking values ± 1 and $r(t) = p(t) \otimes c(t)$. The Fourier transform of $r(t)$ is given by

$$R(f) = C(f)\, P(f) \tag{24}$$

where

$$C(f) = \sum_{k=0}^{K-1} c_k \exp(-\mathrm{j}2\pi k f T) \tag{25}$$

is the transfer function of the encoder and $c(t) = F^{-1}[G(f)]$ is the pulse shaping due to line-coding. The sequence of symbols $\{b_k\}$ is generated to avoid error propagation by a pre-coder defined by

$$a_k = \sum_{i=0}^{K-1} c_i b_{k-i} \bmod (2). \tag{26}$$

The K code coefficients $c_0, c_1, c_2, \ldots, c_{K-1}$ are usually integers and can be properly chosen to generate a specific line-coding scheme (AMI/order-1). It is therefore possible to apply the same procedure for average BER evaluation of CPFSK with NRZ data as in Section 3.1 to the present situation with line-coded data by merely replacing $g_1(t)$ and $g_2(t)$ in the previous case by

$$g_1(t) = \mathrm{Re}[p(t) \otimes c(t) \otimes h_1(t)], \tag{27}$$

$$g_2(t) = \mathrm{Re}[p(t) \otimes c(t) \otimes h_2(t)]. \tag{28}$$

For the line-coded signal, the pulse shaping function $c(t)$ can be obtained from the following $C(f)$ for alternate mark inversion (AMI) and order-1 are given by Equations (29) and (30), respectively,

$$C(f) = 0.5[1 - \exp(-\mathrm{j}2\pi fT)], \tag{29}$$

$$C(f) = \frac{1}{T}[(1+\beta)\cos(\pi fT/2) + (1-\beta)\cos(3\pi fT/2)]^2 \left|S(f)\right|^2, \tag{30}$$

where β is the scaling factor, $c(t) = 1;\ 0 < t < T/2$, and the elementary signals $s_i(t)$ for $i = 1, 2, 3, 4$ in terms of $c(t)$ are given by [19],

$$s_1(t) = c(t) + c(t - T/2), \tag{31}$$

$$s_2(t) = \beta[c(t) - c(t - T/2)], \tag{32}$$

$$s_3(t) = -s_2(t), \tag{33}$$

$$s_4(t) = -s_1(t). \tag{34}$$

4. Results and discussion

Following the analytical formulations, we present the theoretical performance results of an optical CPFSK fiber-optic transmission system with a direct detection receiver for several values of mean DGD with and without line-coding at a bit rate of $10\,\mathrm{Gb\,s^{-1}}$. We assume the worst-case value of power splitting (α) ratio between the two principal states of polarization. The parameters used in computing the BER performance results are shown in Table 1.

The plots of average BER versus optical received power for AMI and order-1 are shown in Figures 2 and 3, respectively, at a modulation index of 0.50 and 1.00. It is observed that the BER performance is more affected at higher values of mean DGD and higher modulation index. From Figure 2, it is also noticed that the BER floor occurs at about 10^{-4} (at DGD 70 ps) and 3.5×10^{-5} (at DGD 60 ps) for AMI and order-1 line-coding, respectively. Above these mean DGD values, the BER can not be lowered by further increasing the signal power.

Table 1. Parameter settings.

Parameter	Values	Unit
Temperature (T)	300	K
Bandwidth (B)	10	GHz
Receiver load (R_L)	50	ohm
Receiver responsivity (R_d)	1	A W^{-1}
Wavelength (λ)	1550	nm
Operating frequency (f)	1.93355×10^{14}	Hz
Scaling factor (β)	0.50	Unitless
Dispersion index (γ)	15	ps $nm^{-1}km^{-1}$
Power splitting ratio (α)	0.50	Unitless

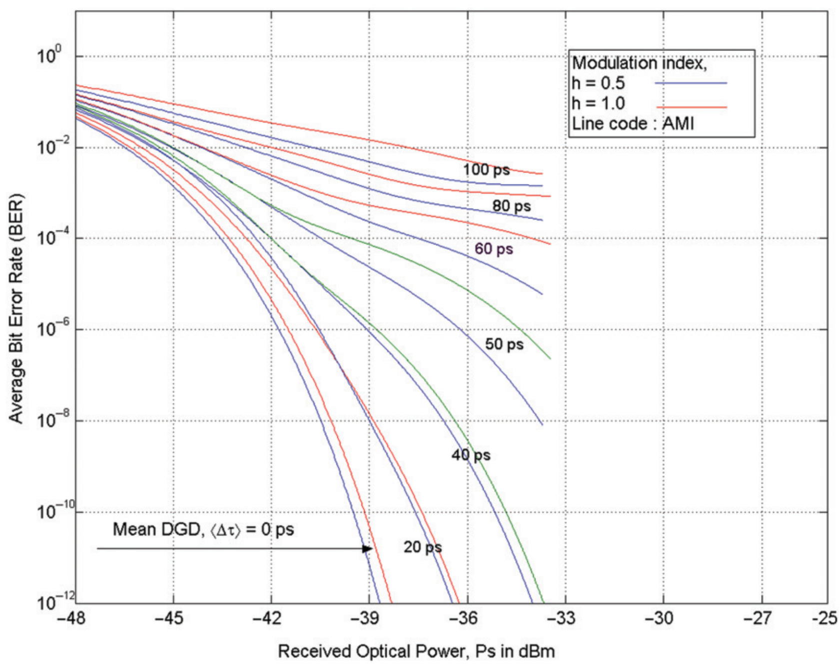

Figure 2. Plots of average BER versus received power with AMI line-coding (modulation index, $h = 0.5$ and $h = 1.0$). (The color version of this figure is included in the online version of the journal.)

It is found from Figures 2 and 3 that the amount of power penalty due to PMD suffered by the CPFSK transmission system up to 30 ps mean DGD is relatively small. For small power penalties PMD follows the following expression [20],

$$\varepsilon \text{ (in dB)} = A\left(\frac{\langle\Delta\tau\rangle}{MT}\right)^2 \alpha(1-\alpha), \tag{35}$$

where α is the power splitting ratio, MT is the symbol duration, A is a dimensionless parameter determined by the pulse shape. In our case, $M = 1$ and the value of A is about 39, 19 and 16 corresponding to NRZ, AMI and order-1 codes, respectively.

Figure 4 shows the 10^{-9} BER power penalty of NRZ-, AMI-, order-1 CPFSK, versus the ratio of mean DGD to bit duration $\langle\Delta\tau\rangle/T$ at a modulation index of 1.0. The performance limitations of an optical direct detection NRZ-CPFSK transmission system affected by PMD is reported in [17]. It is seen that the amount of power penalty improvements are about 1.50 and 2.15 dB corresponding to AMI and order-1, respectively, at mean DGD of 30 ps with respect to NRZ-CPFSK. This is to be expected, because in NRZ, the symbol duration is twice as long as for these line-coding schemes. As these line codes use shorter pulse duration and exhibit much greater PMD tolerance than their NRZ counterparts, it is also observed that order-1 line-coding gives nearly twice the maximum allowable value of $\langle\Delta\tau\rangle/T$ than NRZ data.

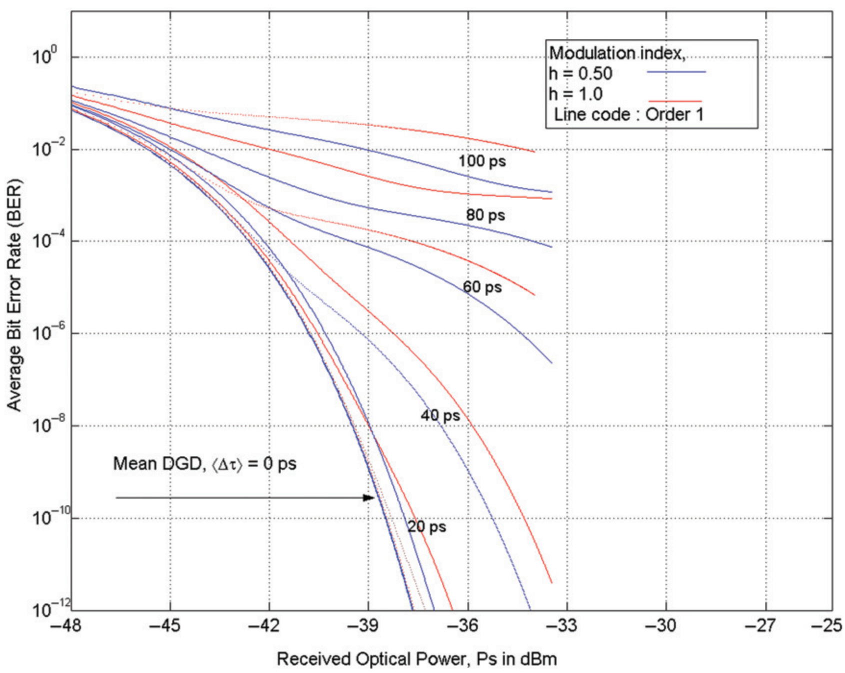

Figure 3. Plots of average BER versus received power with order 1 line-coding (modulation index, $h = 0.5$ and $h = 1.0$). (The color version of this figure is included in the online version of the journal.)

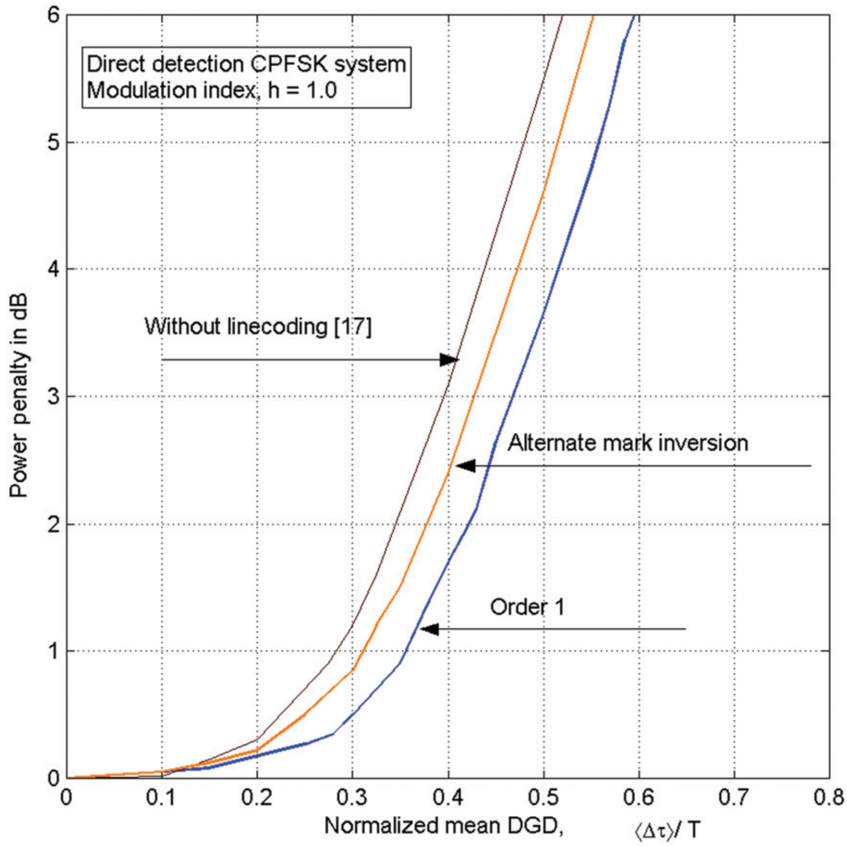

Figure 4. PMD-induced power penalty as a function of DGD/bit duration ($\langle\Delta\tau\rangle/T$) for NRZ-, AMI- and order-1 line-coding of a CPFSK system (modulation index = 1.0). (The color version of this figure is included in the online version of the journal.)

5. Conclusions

We have analytically investigated the performance of two types for line code in terms of BER for PMD tolerance in a CPFSK direct detection optical transmission system and found significant effectiveness in mitigating the PMD impairments in single mode fiber. It is observed that between the two line-coding schemes, order-1 coding exhibits superior performance by 0.65 dB at mean DGD of 30 ps ($h = 1.0$) in the presence of GVD and PMD over that of AMI coding due to its compact spectrum. Thus, the fundamental factor in determining the effectiveness of PMD tolerance is the spectral bandwidth of the transmission signal.

Acknowledgements

This research work has been carried out as part of a PhD thesis work in the Department of Electrical and Electrical Engineering of Bangladesh University of Engineering and Technology (BUET), Dhaka, Bangladesh.

References

[1] Gordon, J.P.; Kogelnik, H.K. *PNAS*. **2000,** *97,* 4541–4550.
[2] Savory, S.J.; Payne, F.P. *J. Lightwave Technol*. **2001,** *19,* 350–359.
[3] Lu, P.; Chen, L.; Bao, X. *J. Lightwave Technol*. **2001,** *19,* 856–860.
[4] Yang, J.; Kath, W.L.; Menyuk, C.R. *Opt. Lett*. **2001,** *26,* 1472–1474.
[5] Karlsson, M.; Brentel, J.; Andrekson, P.A. *J. Lightwave Technol*. **2003,** *18,* 941–951.
[6] Xie, C.; Moller, L. In Evaluation and Mitigation of Polarization Mode Dispersion Impairments in High-speed Transmission Systems, Asia-Pacific Optical Communications (APOC 2006), *Proceedings of the SPIE*, 6353, Korea, Sept 3–7, 2006.
[7] Kaiser, W.; Otte, W.; Wuth, T.; Rosenkranz, W. Experimental Verification of Reduced Sensitivity of Optical Duobinary Modulation to Higher Order PMD. *Proceedings of the Optical Fiber Communication Conference and Exhibit*, Anaheim, CA, Mar 17–22, 2002.
[8] Xie, Y.; Yu, Q.; Yan, L.-S.; Adamczyk, O.H.; Pan, Z.; Lee, S.; Willner, A.E.; Menyuk, C.R. *Proc. OFC* **2001,** *3,* WAA2-1–WAA2-3.
[9] Rao, M.; Li, L.; Tang, Y.; Zhang, M.; Sun, X. *Photon. Network Commun*. **2004,** *7,* 97–104.
[10] Bulow, H.; Thielecke, G. Electronic PMD Mitigation from Linear Equalization to Maximum Likelihood Detection, *Proceedings of the Optical Fiber Communication Conference and Exhibit (OFC 2001)*, Los Angeles, CA, 2001.
[11] Haunstein, H.FW.; Sauer-Greff, W.; Dittrich, A.; Sticht, K.; Urbansky, R. *J. Lightwave Technol*. **2004,** *22,* 1169–1181.
[12] Iwashita, K.; Matsumoto, T. *J. Lightwave Technol*. **1987,** *5,* 452–460.
[13] Wang, J.; Kahn, J.M. *J. Lightwave Technol*. **2004,** *22,* 362–371.
[14] Bedrosian, E.; Rice, S.O. *Proc. IEEE*. **1968,** *56,* 2–13.
[15] Forestieri, E.; Prati, G. *IEEE Select. Areas Commun*. **1995,** *13,* 543–556.
[16] Majumder, S.P.; Gangopadhay, R.; Forestieri, E.; Prati, G. *IEEE Photon. Technol. Lett*. **1995,** *10,* 1207–1209.
[17] Islam, M.S.; Majumder, S.P. *J. Opt. Commun*. **2007,** *20,* 46–51.
[18] Allen, C.T.; Kondamuri, P.K.; Richards, D.L.; Hague, D.C. *J. Lightwave Technol*. **2003,** *21,* 79–86.
[19] Forestieri, E.; Prati, G. *J. Lightwave Technol*. **2001,** *19,* 1675–1684.
[20] Poole, C.D.; Nagel, J. Polarization effects in lightwave systems. In *Optical Fiber Telecommunications*, Vol. III; Kaminow, I.P., Koch, T.L., Eds.; Academic: New York, 1997; Chapter 6.